Threshold for strong thermal dephasing in periodically poled KTP in external cavity frequency doubling

Lundeman, Jesper Holm; Jensen, Ole Bjarlin; Andersen, Peter E.; Petersen, Paul Michael

Published in:
Applied Physics B

Link to article, DOI:
10.1007/s00340-009-3678-6

Publication date:
2009

Document Version
Peer reviewed version

Threshold for strong thermal dephasing in periodically poled KTP in external cavity frequency doubling

Jesper Holm Lundeman*, Ole Bjarlin Jensen, Peter Eskil Andersen, and Paul Michael Petersen

DTU Fotonik, Department of Photonics Engineering, Technical University of Denmark, Frederiksborgvej 399, 4000 Roskilde, Denmark

Corresponding author: jehl@fotonik.dtu.dk

We present a measurements series of the efficiency of periodically poled KTP used for second harmonic generation in an external phase locked cavity. Due to the high absorption ($0.01 cm^{-1}$) in the PPKTP crystal at the pump wavelength a strong thermal dephasing of the periodically poled grating is observed for high pump powers. For four different resonator setups, it was experimentally found that a threshold parameter could be defined as the ratio between the focal intensity in the crystal and the single pass conversion efficiency. The value of this threshold for the onset of strong thermal dephasing was found to be $1.41 \cdot 10^{10}$ W^2m^{-2} in our 30 mm long PPKTP sample. This threshold parameter marks the onset of thermally induced instability that leads to a degradation of the SHG conversion efficiency. Above the threshold the shape of the resonance peaks of the resonator changed from symmetrical into triangular making phase locking difficult.

PACS numbers: 42.55.Px, 42.65.Ky, 42.65.Pc, 42.70.Mp,

1. Introduction

Periodically poled nonlinear crystals are commonly employed for second harmonic generation (SHG) of near infrared light sources into the visible range [1-4]. For development of a light source emitting at 400 nm, several different nonlinear materials can be used. Periodically poled Lithium Niobate (PPLN) and periodically poled Lithium Tantalate (PPLT) both offer high effective nonlinearities (16 pm/V and 10 pm/V) and modest absorption at 800 nm. However, both PPLN and PPLT suffer from photorefractivity, and hence make them unsuitable for intracavity SHG applications in the visible spectral range. Periodically poled KTP (PPKTP) does not experience photorefractivity, has only a slightly lower figure of merit (d_{eff}^2 / n^3) than PPLN and a higher absorption at both the fundamental and second harmonic wavelength, respectively. The larger apertures available with PPKTP crystals, due to easier manufacturing of short domains, also minimize the diffractive coupling losses. Another important material group for SHG is the borates (LBO, BBO, BiBO), but these suffer from walk-off, reducing the overall beam-quality. Despite the lower nonlinearity and higher absorption of PPKTP, we have chosen to use PPKTP in this work.

The absorption of light at the second harmonic at 404 nm in KTP is on the order of 0.1-0.2 cm^{-1}[5] and the absorption of light at the 808 nm pump in our crystal was measured to be 0.01 cm^{-1}. The latter was determined in our crystal by both a direct transmission experiment and from finesse measurements of the external resonator. Several authors [1-4] have reported on thermal issues with high input powers in periodically poled crystals, due to absorption, but to our knowledge not for wavelengths lower than 423 nm.

In this paper we report on the measurements of strong thermal loading of the crystal. We have employed the use of four different external resonators, in order to experimentally investigate the optimum spot size in the crystal that yields the highest cw frequency doubled output power in a diffraction limited beam. We experimentally found that the transition from the quadratic dependence of the second harmonic power on the pump power into the less

efficient strong thermal dephasing regime, could be obtained from the ratio between the focal intensity in the crystal and the single pass conversion efficiency.

2. Experimental setup

The experimental setup, shown in fig. 1, is based on the same configuration that we reported in [6] with the pump source of similar design as reported in [7]. The laser output was 1.4 W measured before the isolator, and 1.2 W at the input of the external doubler resonator. The beam quality parameter M^2 was measured to be <1.3 for both axes.

The external resonator is consisting of only two spherical mirrors, and a Brewster cut crystal for second harmonic generation. This configuration allows for very compact setups, with a short optical path length and good mechanical stability. The four setups each used a different set of spherical mirrors in order to vary the beam waist in the crystal, all with approximately the same ellipticity. In order to adjust the roundtrip length of the resonator, one of the mirrors is mounted on a piezo, and used in the polarization locking scheme [8]. The input mirror was 85 % reflective, while the piezo mounted mirror was highly reflective for 810 nm and anti-reflection coated for 405 nm allowing for it to serve as output coupler. The data describing the four different setups are summarized in table 1. For comparison, the optimal beam waist for a 30 mm long crystal is 27 μm, resulting in a conversion efficiency of 3.3 %/W according to Boyd-Kleinman theory [9].

The second harmonic conversion efficiencies η were measured in single pass through the crystal after being placed inside the external resonator and optimized for largest scanning mode SH output. The generated blue power was measured as a function of crystal temperature and fitted with a sinc^2 function from which the temperature bandwidth T_{FWHM} = 0.44 K of the crystal was obtained. The temperature delta is the difference in temperature between scanning mode operation of the cavity and the stable cw mode. As the temperature

delta is larger than T_{FWHM} it is necessary to decrease the crystal temperature when changing from scanning mode to cw mode.

3. Results

The experimental work for the resonator was carried out with the aim of maximizing the extracted power in the second harmonic beam. All power levels reported for the second harmonic beam are measured after exiting the resonator. By measuring the leaked beam through the piezo mirror, the circulating power can be deduced, and the magnitude of the dip in the reflection from the input mirror when the system is on resonance, is a measure of the coupling efficiency into the resonator.

3.1. Second harmonic efficiency

The generated powers in cw and scanning modes are shown in fig. 2 as a function of circulating power. A quadratic fit of the form of $P_{SH} = \eta P_{circ}^2$ shows good agreement with the scanning mode experimental results. The coupling efficiency is smaller in cw mode than in scanning mode, which is attributed to a thermal lens generated inside the crystal that changes the eigenmode of the resonator. The mode matching was optimized in the scanning mode, away from thermal equilibrium, contrary to the cw mode, where the temperature distribution will change to the steady state solution and thereby create a thermal lens. In general the coupling efficiency in scanning mode is 80 %, and decreases to 60 % in cw mode. The largest cw power of 320 mW was obtained when using the 52 mm mirrors, see Table 1. The general uncertainties of the measurements are estimated to be less than 10 %.

From fig. 2 it can be seen that for a certain power level in the crystal the generated cw second harmonic power starts to deviate from the quadratic fit, and eventually becomes close to linear. This point marks the onset of strong thermal dephasing, and in the case of the 26

mm setup, occurs when the second harmonic power has dropped to 83% of the calculated power.

We define the ratio between the pump beams focal intensity I_f in the crystal and the single pass conversion efficiency as

$$K = P_c / \pi w_x w_y \eta = I_f / \eta \qquad (1)$$

with P_c being the circulating power and w_x *and* w_y the waists of the beam inside the crystal. When calculating the K value for all four resonator setups, using a circulating power yielding 83% of the expected power, we obtain a threshold constant $K_T = 1.41 \cdot 10^{10} \pm 0.02$ $W^2 m^{-2}$.

A plot of K as a function of the ratio γ between the measured second harmonic power and the calculated parabolic fit is shown in fig. 3. Around the value γ = 0.83 these curves can be seen to have an inflection point, marking the onset of strong thermal dephasing. The power P_c satisfying (1) is thus called the threshold power. Experimentally we observe that the K-value for each of the four setups are very similar. This leads to the important and interesting result that one can obtain the optimum output power taking into account the trade-off between conversion efficiency and thermal effects for a single (arbitrary) configuration.

Based on the cylindrical heat transfer equation [10] the calculated temperature rise at this threshold power level in the crystal, were found to be within 0.03 K of the measured temperature bandwidth T_{FWHM} of the crystal (0.44 K). We therefore believe that this simple procedure can be used to estimate when thermal effects are starting to seriously degrade the performance of the nonlinear crystal. For circulating powers below the threshold, the SH power is following the simple parabolic dependence of the pump power. Above threshold the temperature difference inside the crystal becomes larger than the T_{FWHM} of the crystal. This effectively shortens the interaction length inside the crystal, due to non-optimal phase matching. The domain of weak thermal dephasing can be modeled like ref. [4], whereas the

strong dephasing with a large local temperature gradient must be solved with the fully coupled equations [11].

The numerical value of the threshold for strong thermal dephasing, found in this work, is only applicable to our KTP crystal, and will in general be dependent on the chosen crystal material, the interaction wavelengths and sample purity. However, we believe the relation can be extended to other materials, like PPLN and PPLT.

3.2. Self-locking

Several authors have reported on self-locking in different materials [1,2,10]. This effect can be seen when scanning the resonator, as asymmetrical peaks depending on the scan direction of the piezo. This is caused by the heating of the crystal which due to thermal expansion changes the phase of the circulating beam. The result is that when the optical path length is decreased by moving the piezo, the optical length of the crystal increases. This effect makes the peaks in the scanning mode spectrum asymmetrical and triangular for large absorbed powers. We have measured these peaks at a scan rate of 1 Hz, resulting in 1 free spectral range to be swept in 250 ms which is considerably slower than the relaxation time of the crystal, thereby creating quasi-cw conditions in the crystal. The measured resonance peaks for the 39 mm setup are shown in fig. 4, and clearly show the peaks becoming asymmetrical and then triangular with increasing circulating power. Around the critical input power (P_c = 3.4 W) the peak shape changes into the triangular shape. It can be difficult to lock the setup under these conditions, using the polarization locking scheme, as the piezo can only be moved in one direction, while maintaining phase-match.

4. Conclusion

In conclusion we have investigated four external cavities for second harmonic generation of 404 nm. Each resonator was constructed with a different set of spherical

mirrors, in order to vary the spot size inside the PPKTP crystal. With a coupled power of 630 mW a spot size of 3-4 times the optimal size dictated by Boyd-Kleinman theory was found to generate the largest amount of second harmonic ouput power. At this pump power level the coupling efficiency changed from 80 % in scanning mode to 60 % in cw mode due to thermal lensing in the crystal. It was experimentally found that a threshold parameter K_T could be defined as the ratio between the focal intensity I_f in the crystal and the single pass conversion efficiency η. The value of this threshold parameter for the onset of strong thermal dephasing was found to be $1.41 \cdot 10^{10}$ W^2m^{-2} in our sample. The corresponding rise in crystal temperature at this power level was found to equal the measured temperature bandwidth T_{FWHM}. We also found a change in the shape of the resonance peaks when scanning the resonator slowly, and above the threshold value the polarization locking was difficult.

The authors acknowledge the financial support from the BIOPHOT programme (Danish Research Agency FTP, grant 26-02-0020) and EU-FP6 integrated project WWW.BRIGHTER.EU contract IST-2005-035266.

1. F. Torabi-Goudarzi and E. Riis, *Efficient cw high-power frequency doubling in periodically poled KTP*, Opt. Comm. **227**, 389-403 (2003).
2. R. Le Targat, J.-J. Zondy, and P. Lemonde, *75%-Efficiency blue generation from an intracavity PPKTP frequency doubler*, Opt. Comm. **247**, 471-481 (2005).
3. F. J. Kontur, I. Dajani, Y. Lu, and R. J. Knize, *Frequency-doubling of a CW fiber laser using PPKTP, PPMgSLT, and PPMgLN*, Opt. Expr. 15, 12882-12889 (2007).
4. Z. M. Liao, S. A. Payne, J. Dawson, A. Drobshoff, C. Ebbers, D. Pennington, and L. Taylor, *Thermally induced dephasing in periodically poled KTP frequency-doubling crystals*, J. Opt. Soc. Am. B. **21**, 2191-2196 (2004).

5. G. Hansson, H. Karlsson, S. Wang, and F. Laurell, *Transmission Measurements in KTP and Isomorphic Compounds*, Appl. Opt. **39**, 5058-5069 (2000).
6. J. H. Lundeman, O. B. Jensen, P. E. Andersen, S. Andersson-Engels, B. Sumpf, G. Erbert, and P. M. Petersen, *High power 404 nm source based on second harmonic generation in PPKTP of a tapered external feedback diode laser*, Opt. Exp. **16**, 2486-2493 (2008).
7. M. Chi, O. B. Jensen, J. Holm, C. Pedersen, P. E. Andersen, G. Erbert, B. Sumpf, and P. M. Petersen, *Tunable high-power narrow-linewidth semiconductor laser based on an external-cavity tapered amplifier*, Opt. Exp. **13**, 10589-10596 (2005).
8. T. W. Hänsch and B. Couillaud, *Laser frequency stabilization by polarization spectroscopy of a reflecting reference cavity*, Opt. Comm. **35**, 441-444 (1980).
9. G. D. Boyd and D. A. Kleinman, *Parametric Interaction of Focused Gaussian Light Beams*, J. Appl. Phys. **39**, 3597-3639 (1968).
10. M. E. Innocenzi, H. T. Yura, C. L. Fincher, and R. A. Fields, *Thermal modelling of continous-wave end-pumped solid-state lasers*, Appl. Phys. Lett. **56**, 1831-1833 (1990).
11. O. A. Louchev, N. E. Yu, S. Kurimura, and K. Kitamura, *Thermal inhibition of high-power second-harmonic generation in periodically poled $LiNbO_3$ and $LiTaO_3$ crystals*, Appl. Phys. Lett. **87**, 131101 (2005).

Figure Captions:

1. The experimental setup used. For the 52 mm and 100 mm setups, the SH beam can exit the resonator directly. HWP – half wave plate, PPKTP – periodically poled KTP crystal.
2. The second harmonic generated power as a function of the circulating intracavity pump power. The full (red) line is the calculated line based on the single pass conversion efficiency η. Diamonds - scanning mode results, squares – locked cw results.
3. The *K* value plotted as function of the ratio between measured and calculated second harmonic power γ. The grey dashed line indicates the inflection point.
4. The resonance peak shapes, for different circulating powers in the 39 mm cavity.

Table Captions:

1. The main attributes of the four different resonator setups.

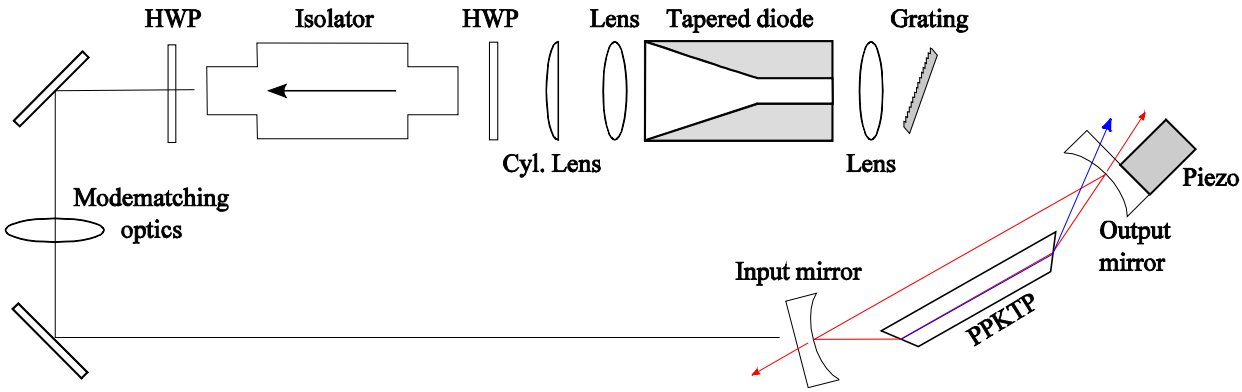
HWP
Isolator
HWP
Lens
Tapered diode
Grating
Cyl. Lens
Lens
Piezo
Modematching
optics
Output
mirror
Input mirror
PPKTP

Figure 1

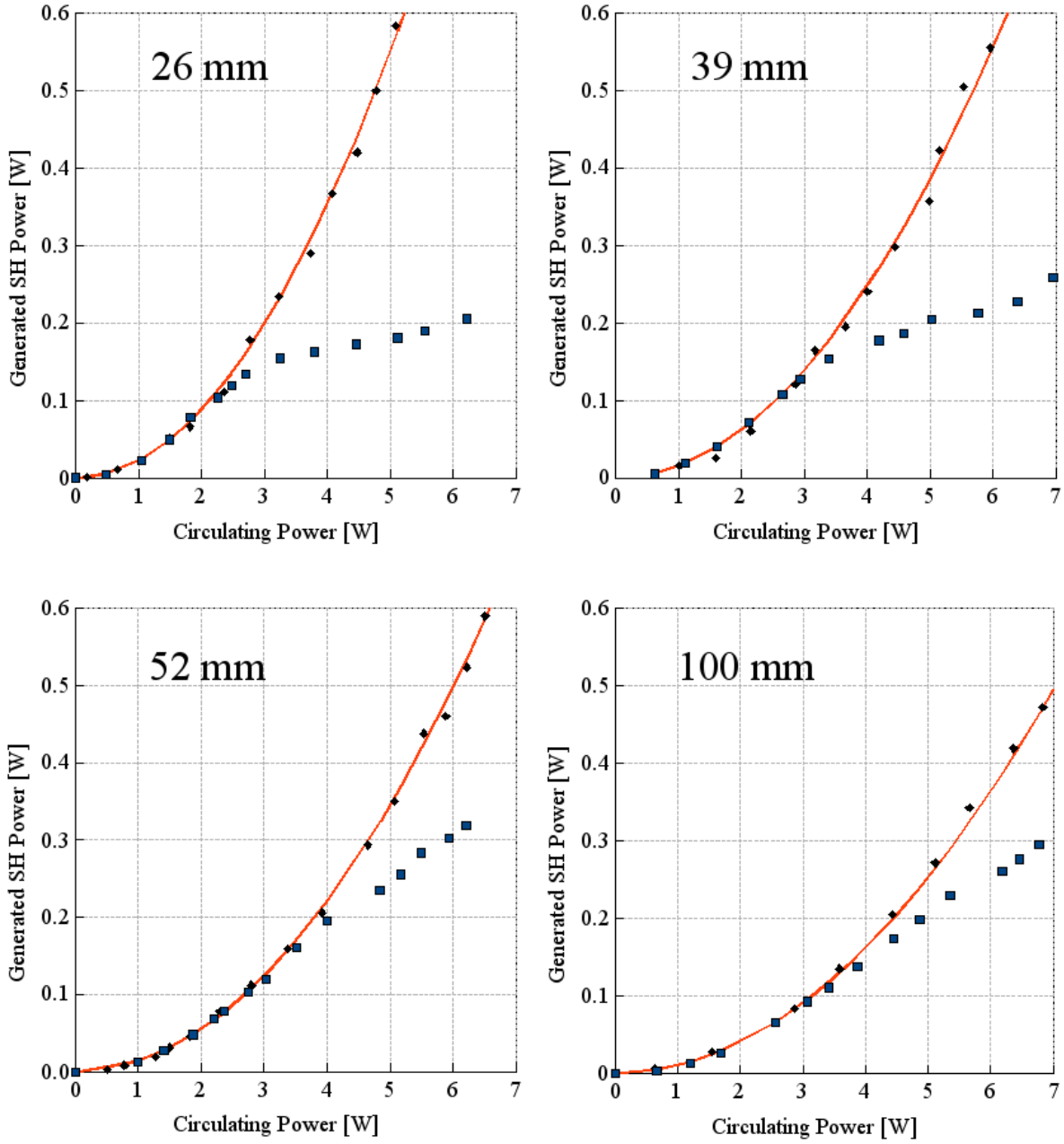
26 mm
39 mm
52 mm
100 mm
Generated SH Power [W]
Circulating Power [W]
0.0
0.1
0.2
0.3
0.4
0.5
0.6
0
1
2
3
4
5
6
7

Figure 2

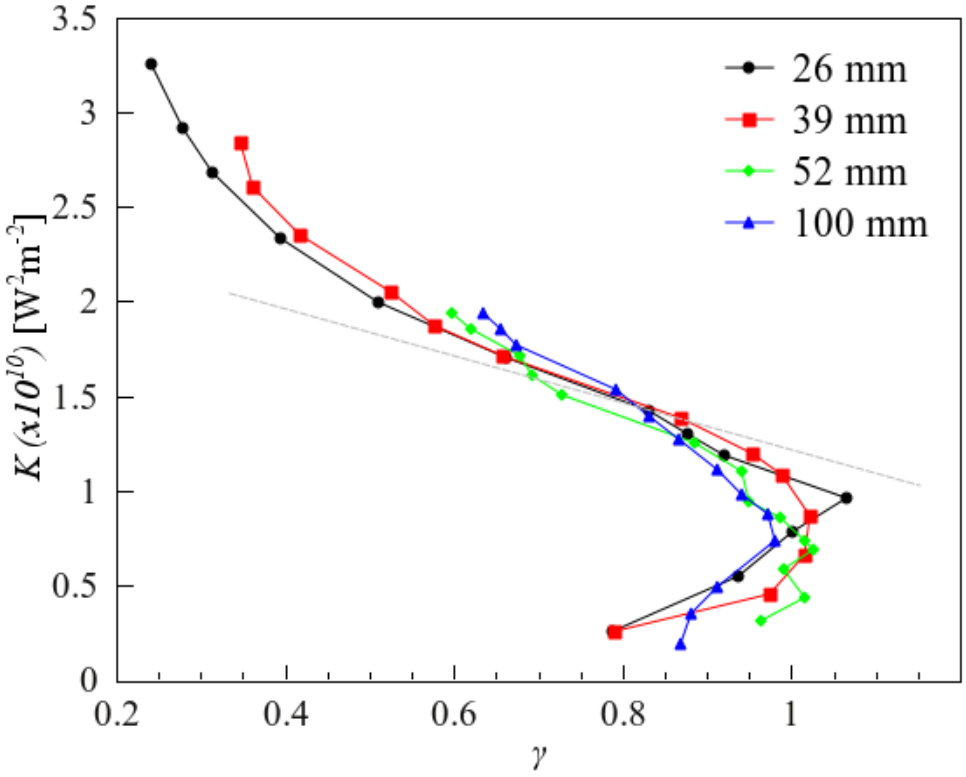

Figure 3

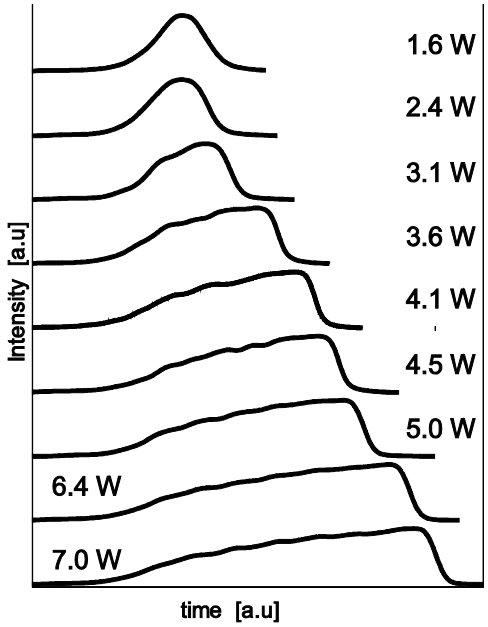

Figure 4

Attribute	**Unit**				
Mirror ROC	mm	26	39	52	100
Length	cm	12.8	15.4	17.7	42.2
Line width	MHz	67	56	48	20
Beamwaist X	µm	60	83	100	121
Beamwaist Y	µm	46	61	74	91
Absorption at 808nm	%	2.9	2.8	3.1	3.0
SH conv. eff.	% / W	2.20	1.54	1.38	1.01
T_{FWHM}	K	0.45	0.43	0.44	0.43
Temp. delta	K	2.2	1.6	1.3	1.0
Max cw Power at 404 nm	mW	205	258	318	295
Max scanning Power at 404 nm	mW	729	679	622	518
K-value (for $\gamma = 0.83$)	W^2m^{-2}	$1.42 \cdot 10^{10}$	$1.43 \cdot 10^{10}$	$1.39 \cdot 10^{10}$	$1.39 \cdot 10^{10}$

Table 1: The main attributes of the four different resonator setups.